

Constraints on the Circumstellar Disk Masses in the IC 348 Cluster

John M. Carpenter

*California Institute of Technology, Department of Astronomy, MS 105-24,
Pasadena, CA 91125; email: jmc@astro.caltech.edu*

ABSTRACT

A $5.2' \times 5.2'$ region toward the young cluster IC 348 has been imaged in the millimeter continuum at $4.0'' \times 4.9''$ resolution with the OVRO interferometer to a RMS noise level of $0.75 \text{ mJy beam}^{-1}$ at 98 GHz. The data are used to constrain the circumstellar disk masses in a cluster environment at an age of ~ 2 Myr. The mosaic encompasses 95 known members of the IC 348 cluster with a stellar mass distribution that peaks at 0.2 - $0.5 M_{\odot}$. None of the stars are detected in the millimeter continuum at an intensity level of 3σ or greater. The mean observed flux for the ensemble of 95 stars is $0.22 \pm 0.08 \text{ mJy}$. Assuming a dust temperature of 20 K, a mass opacity coefficient of $\kappa_o = 0.02 \text{ cm}^2 \text{ g}^{-1}$ at $1300 \mu\text{m}$, and a power law index of $\beta = 1$ for the particle emissivity, these observations imply that the 3σ upper limit to the disk mass around any individual star is $0.025 M_{\odot}$, and that the average disk mass is $0.002 \pm 0.001 M_{\odot}$. The absence of disks with masses in excess of $0.025 M_{\odot}$ in IC 348 is different at the $\sim 3\sigma$ confidence level from Taurus, where $\sim 14\%$ of the stars in an optically selected sample have such disk masses. Compared with the minimum mass needed to form the planets in our solar system ($\sim 0.01 M_{\odot}$), the lack of massive disks and the low mean disk mass in IC 348 suggest either that planets more massive than a few Jupiter masses will form infrequently around 0.2 - $0.5 M_{\odot}$ stars in IC 348, or that the process to form such planets has significantly depleted the disk of small dust grains on time scales less than the cluster age of ~ 2 Myr.

Subject headings: stars:pre-main-sequence — stars:disks — open clusters and associations

1. Introduction

High resolution imaging at optical, near-infrared, and millimeter-wave wavelengths have conclusively demonstrated that circumstellar disks are ubiquitous around young solar-mass stars (O'Dell & Wong 1996; Padgett et al. 1999; Dutrey et al. 1996). The long-held notion that planets may frequently form in these disks has been dramatically confirmed with the increasing number of planets detected around nearby main-sequence stars (Marcy, Cochran, & Mayor 2000). While a consensus has not yet been reached on how planets form in circumstellar disks, current theories propose that gas-giant planets form either as gravitational instabilities in an accretion disk (Boss 2001), or from

the more gradual build up of planetesimals to form a rocky core followed by accretion of gaseous material (Pollack et al. 1996). In both class of models, the accretion disk lifetime sets an important time scale on the planet formation process by constraining the time available for a gravitational instability to develop or the rocky core to form before the gas and dust are dissipated.

Circumstellar accretion disks around young stars are commonly inferred based on the presence of infrared emission in excess of the stellar photosphere. In many stars the excess infrared emission from $1\text{-}100\mu\text{m}$ can be modeled with a geometrically thin, optically thick accretion disk (Lynden-Bell & Pringle 1974), although inner disk holes, flaring, and other refinements to this basic model are often needed to reproduce the observations in detail (Adams, Shu, & Lada 1988; Calvet et al. 1991,92; Chiang & Goldreich 1997). Detailed spectral energy distributions from the near- to far-infrared have been compiled for only a few nearby star forming regions (e.g. Strom et al. 1989; Wilking, Lada, & Young 1989), but J -, H -, K -, and L -band imaging studies provide an efficient means to search for near-infrared excesses in hundreds of stars (often in clusters) of various ages. Recent results indicate that at least 50% of solar mass stars at an age of ~ 1 Myr exhibit a near-infrared excess, but that the percentage decreases to $\lesssim 10\%$ for ages 3-10 Myr (Strom et al. 1989; Haisch, Lada, & Lada 2001b). These results are consistent with the notion that the lifetime of accretion disks around most solar mass stars is $\sim 3\text{-}10$ Myr.

Strictly speaking, a near-infrared excess is diagnostic of only hot dust with temperatures of ~ 1000 K. For a solar mass star, these temperatures are found only within ~ 0.1 AU of the star. Most of the dust mass, and presumably the majority of planet formation, will be located at larger radii and have temperatures too cool to radiate in the near-infrared. Further, some disks are thought to have inner holes such that stars without near-infrared excesses may still contain substantial disk masses. (Although $10\mu\text{m}$ observations suggest that the transition from an optically thick to an optically thin disk occurs on time scales of ~ 0.3 Myr, in which case near-infrared observations may in fact provide an indirect probe of the larger scale disk; Skrutskie et al. 1990, see also Haisch, Lada, & Lada 2001a). An additional limitation of near-infrared studies is that the emission is optically thick and provides little meaningful constraints on the disk mass (see, e.g., Wood et al. 2002). Longer wavelength observations are needed to establish the disk lifetime at large orbital radii and to provide measures on how disk masses evolve with time.

Millimeter and submillimeter continuum emission are the best available tracers of dust in the cool, outer disk. The most comprehensive continuum surveys to date have been toward young stars in Taurus (Beckwith et al. 1990; Osterloh & Beckwith 1995; Motte & André 2001), ρ Oph (André & Montmerle 1994; Nürnberger et al. 1998; Motte, André, & Neri 1998), Lupus (Nürnberger, Chini, & Zinnecker 1997), Chamaeleon I (Henning et al. 1993), and Serpens (Testi & Sargent 1998). These observations have shown that at an age of ~ 1 Myr, $\sim 20\text{-}30\%$ of the stars possess a circumstellar disk with a mass greater than the minimum mass of the solar nebula ($\sim 0.01 M_\odot$; Weidenschilling 1977, Hayashi 1981), and that the median disk mass is $\lesssim 0.004 M_\odot$. Further insights into disk evolution can be obtained by using rich clusters as a tool to empirically measure the mass of disks as a function of stellar mass and age in much the same manner near-infrared studies have used clusters

to establish the frequency of inner accretion disks (Haisch, Lada, & Lada 2001b). Continuum surveys of clusters are also important since an appreciable fraction of stars in molecular clouds are found in rich clusters (Lada et al. 1991; Carpenter 2000), and the high ultraviolet radiation fields produced by O-stars in clusters may influence disk evolution (Johnstone, Hollenbach, & Bally 1998; Störzer & Hollenbach 1999; Scally & Clarke 2001).

The main observational challenge to studying clusters in the millimeter continuum is that high angular resolution is required to resolve the stars and distinguish disk emission from the more extended molecular cloud. The only rich cluster surveyed to date by interferometric techniques has been the Orion Nebula Cluster (Mundy, Looney, & Lada 1995; Bally et al. 1998). However, these observations were 10-50 times less sensitive to dust mass than the observations of Taurus and ρ Oph and did not place stringent limits on the amount of circumstellar mass around individual stars. Given the limitations in inferring disk evolution from near-infrared excesses, it is important to conduct millimeter continuum observations of additional star forming regions in order to understand the evolution of disk masses at young stellar ages when planets are in their formative stages.

To further measure the circumstellar disk masses in different star forming environments, I obtained $\lambda 3\text{mm}$ continuum observations of the young cluster IC 348 with the OVRO millimeter wave interferometer. Based on statistical analysis of near-infrared star counts, the IC 348 cluster contains ~ 400 stars distributed over a $\sim 20' \times 20'$ region ($1.9 \text{ pc} \times 1.9 \text{ pc}$ at the assumed distance of 320 pc; de Zeeuw et al. 1999; Herbig 1998), with about half the stars located within the central $7' \times 7'$ region (Lada & Lada 1995; Carpenter 2000). To date, ~ 200 stars and brown dwarfs have been individually identified as likely cluster members based on their spectroscopic and photometric properties (Herbig 1998; Luhman et al. 1998; Luhman 1999; Najita, Tiede, & Carr 2000), and 115-173 likely members have been detected with x-rays (Preibisch & Zinnecker 2001). A cluster age of ~ 2 Myr (Luhman 1999; see also Herbig 1998) has been inferred by placing the low mass stars on the HR diagram and using theoretical pre-main-sequence evolutionary tracks from D'Antona & Mazzitelli (1997,98). Near-infrared imaging surveys of the cluster show that $\sim 65\%$ of the stars contain a $K - L$ excess characteristic of an optically thick accretion disk (Lada & Lada 1995; Haisch, Lada, & Lada 2001a). By mosaicking the central $5.2' \times 5.2'$ region ($0.48 \text{ pc} \times 0.48 \text{ pc}$) of the IC 348 cluster in the millimeter continuum, I investigate the circumstellar disk masses in 95 known cluster members.

The OVRO observations of the IC 348 cluster are described in Section 2. The stellar properties of the cluster members within the OVRO mosaic boundaries are reviewed in Section 3, and constraints on the circumstellar disk masses are derived in Section 4. Section 5 compares these results with disk masses in Taurus and the Orion Nebula Cluster, and discusses the implications for planet formation. The conclusions are summarized in Section 6.

2. OVRO Observations

A $5.2' \times 5.2'$ region toward the IC 348 cluster was mosaicked in the $\lambda 3\text{mm}$ continuum using the OVRO millimeter-wave interferometer between September 2001 and January 2002. Continuum data were recorded simultaneously in four, 1 GHz wide continuum channels centered at 96.48 GHz, 97.98 GHz, 100.98 GHz, and 102.48 GHz. The phase and amplitude calibrator was J0336+323 ($\alpha, \delta = 03:36:30.10, +32:18:29.3$ J2000), which is located 1.7° from the cluster center. The data were calibrated using the OVRO MMA data reduction package (Scoville et al. 1993). The adopted continuum flux for J0336+323, calibrated by observing Neptune and/or Uranus, was 1.60 Jy. The RMS dispersion in the measured flux for J0336+323 is 0.10 Jy as computed from observations on 12 separate nights in which both the calibrator and the planets were observed.

The mosaic consists of 64 pointing centers arranged in a 8×8 grid as shown in Figure 1. The pointing centers along a row are separated by $40''$ (compared to the primary FWHM beam size of $72''$). Adjacent rows are also separated by $40''$ but with pointing centers shifted by $20''$ in right ascension. The mosaicking sequence consisted of obtaining a 3 minute integration on the phase calibrator followed by observing 5 positions in the mosaic for 3 minutes each. This sequence was repeated until all 64 positions in the mosaic were observed. The mosaic was observed in the OVRO compact, low, equatorial, and high configurations both to increase the UV sampling and to decrease the RMS noise. The top few rows in the mosaic were often observed at high airmass with lower sensitivity. Additional observations of these rows were obtained to provide more uniform sensitivity across the mosaic.

The 64 individual points were formed into an image using the mosaicking routines in MIRIAD. The data were averaged using natural weighting to maximize sensitivity, resulting in a beam size of $4.0'' \times 4.9''$. Unit gain was achieved over a $\sim 5.2' \times 5.2'$ area as shown by the dotted curve in Figure 1. The average RMS noise within the unit gain region is $0.75 \text{ mJy beam}^{-1}$ and is spatially uniform over the mosaic to within 10%.

3. The IC 348 Cluster

Before using the OVRO observations to constrain the circumstellar disk masses in the IC 348 cluster, I review the stellar properties of the IC 348 cluster members located within the mosaic boundaries. The stellar and substellar membership list of the IC 348 cluster was compiled from the spectroscopic observations by Herbig (1998), Luhman et al. (1998), and Luhman (1999), and the narrow band imaging survey by Najita, Tiede, & Carr (2000). To ensure a reliable list of cluster members, only sources brighter than $K_s=14.5$ were considered cluster members for this study, as the field star contamination becomes appreciable at fainter magnitudes (Luhman et al. 1998; Najita, Tiede, & Carr 2000). In total, 95 cluster members brighter than $K_s=14.5$ have been identified within the OVRO mosaic. Astrometry for these sources was adopted from 2MASS. The astrometric uncertainty ($\lesssim 0.2''$) is 20 times less than the synthesized beam size.

Stellar masses and ages for 92 of the 95 cluster members have been estimated using the D'Antona & Mazzitelli (1997,98) theoretical pre-main-sequence evolutionary tracks and published spectroscopic and photometric data as described in Hillenbrand, Meyer, & Carpenter (2002). Three sources do not have mass estimates since optical photometry is not available, or in one case, the spectral type could not be determined since the source is possibly a Class I object (Luhman et al. 1998). Figures 2 and 3 show histograms of the inferred stellar masses and ages respectively. (Also shown in these figures are the stellar mass and age histograms for a subsample of the Taurus population as discussed in Section 5.) The stellar masses range from $0.03 M_{\odot}$ to $4.2 M_{\odot}$ with a broad peak in the distribution at about $0.2\text{--}0.5 M_{\odot}$. The mean age of the stellar population is ~ 2 Myr. The properties of this subsample agree well with the properties of the entire IC 348 population identified so far (Herbig 1998; Luhman et al. 1998; Luhman 1999).

To investigate the frequency distribution of inner accretion disks in this subsample of the IC 348 cluster, Figure 4 shows the $J - H$ vs. $H - K_s$ and $J - H$ vs. $K_s - L$ color-color diagrams. The J , H , and K_s photometry are from 2MASS, and the L -band photometry is from Haisch, Lada, & Lada (2001a). Only sources with no processing flags in the 2MASS database are shown. In Figure 4, the solid curves represent the locus of main-sequence and giant stars (Bessell & Brett 1988) and the dashed line is the interstellar reddening vector (Cohen et al. 1981), where the $J - H$ and $H - K$ colors have been transformed into the 2MASS photometric system (Carpenter 2001). Of the 82 sources in the $J - H$ vs. $H - K_s$ diagram, 4 have near-infrared colors to the right of the reddening vectors that are consistent with an infrared excess. However, for each of these four stars, the magnitude of the apparent $H - K_s$ excess is less than the 1σ photometric uncertainties and therefore may be attributed to photometric noise. The fraction of stars with an infrared excess is higher in the $J - H$ vs. $K_s - L$ diagram since L -band shows larger contrast between the disk and photospheric emission. Of the 47 stars with available J , H , K_s , and L -band photometry, 18 (38%) contain an apparent $K_s - L$ excess. Haisch, Lada, & Lada (2001a) do not report L -band photometric uncertainties for individual sources. Based on the distribution of stars blueward of the un-reddened main-sequence in the $J - H$ vs. $K_s - L$ diagram (a region which cannot be populated except from photometric noise and photometric variability between the time of the 2MASS and L -band observations), I estimate that ~ 4 sources may have an apparent $K_s - L$ excess due to noise. Therefore, a minimum of $\sim 15\%$ of the 95 IC 348 members within the OVRO mosaic have near-infrared colors indicative of an optically thick, inner accretion disk. By comparison, Haisch, Lada, & Lada (2001a) estimate that the $\sim 65\%$ of the stars in the IC 348 cluster brighter than $K=12$ have a $K - L$ excess.

4. Constraints on Disk Masses

Figure 5 shows gray scale and contour maps of the OVRO mosaic. In the contour map, the dotted curve shows the unit gain boundary of the mosaic, and the open circles indicate the positions of the 95 known members of the IC 348 cluster within the unit gain boundary. The contours begin

at 3σ above the RMS noise of $0.75 \text{ mJy beam}^{-1}$ with increments of 1σ . Visual inspection of the contour map shows that none of the known IC 348 cluster members have been detected in the $\lambda 3\text{mm}$ continuum at the 3σ level or greater. Over the entire mosaic, the brightest observed flux is only 3.9σ above the noise, and the frequency distribution of fluxes are consistent with gaussian noise as shown by the solid circles in Figure 6. Therefore there are no definitive continuum detections in the mosaic.

Circumstellar disks in Taurus typically have diameters of $\lesssim 300 \text{ AU}$ as measured in the $\lambda 3\text{mm}$ continuum (Dutrey et al. 1996). Assuming that the disks in IC 348 are similar, the disks can be considered point sources at the resolution of these observations ($1600 \text{ AU} \times 1300 \text{ AU}$) when computing upper limits to the continuum flux. A histogram of the observed fluxes toward the 95 cluster members is shown in Figure 6. The dotted line through the histogram shows the expected flux distribution for gaussian noise given the observed RMS noise of $0.75 \text{ mJy beam}^{-1}$. The observed mean flux toward the cluster members is $0.22 \pm 0.08 \text{ mJy}$, where the uncertainty represents the standard deviation of the mean of the 95 cluster members. These results indicate that while the flux distribution is consistent with gaussian noise, there is a positive bias to the average flux at the 2.8σ confidence level.

The OVRO continuum observations can be used to place constraints on the circumstellar disk masses. In reality, most disks will contain a range of dust temperatures with decreasing temperatures with increasing radial distance from the star. The data obtained here do not permit sophisticated modeling of the disk structure, however, and a single dust temperature was assumed. Following Hildebrand (1983), the disk mass (i.e. sum of the dust and gas components) can then be estimated as $M_{disk} = \frac{S_\nu D^2}{\kappa_\nu B_\nu(T_{dust})}$, where $\kappa_\nu = \kappa_o (\frac{\nu}{\nu_o})^\beta$ is the mass opacity coefficient, β parameterizes the frequency dependence of κ_ν , S_ν is the observed flux, T_{dust} is the dust temperature, and $B_\nu(T_{dust})$ is the Planck function. For consistency with prior studies, I assumed $\beta=1.0$ and $\kappa_o = 0.02 \text{ cm}^2 \text{ g}^{-1}$ at $1300\mu\text{m}$ (Beckwith et al. 1990). The value of κ_o , and consequently the disk masses, is uncertain by at least a factor of three (Beckwith et al. 1990). The power law index β may be as low as ~ 0.5 on average in circumstellar disks (Beckwith & Sargent 1991; Mannings & Emerson 1994). If this lower value of β is more appropriate for circumstellar disks, the assumptions adopted here will overestimate the disk masses by 50%.

The appropriate dust temperature for calculating the disk masses was estimated using the circumstellar disk models from Beckwith et al. (1990) and Osterloh & Beckwith (1995). These studies fitted radial power-law distributions for the dust temperature and disk mass surface density to the observed infrared and millimeter spectral energy distribution for well-studied stars in Taurus-Auriga. From the disk mass derived by these model fits, I computed a single component dust temperature for each star that reproduces the disk mass given the observed $\lambda 1.3\text{mm}$ flux. A histogram of these ‘effective’ dust temperatures is shown in Figure 7. (Four stars with effective temperatures greater than 100 K are not shown in this figure.) Of the 44 stars in Taurus-Auriga with model disk masses from Beckwith et al. (1990) and Osterloh & Beckwith (1995), the median dust temperature derived in this manner is $\sim 20 \text{ K}$. If this dust temperature is then assumed for

all of the Taurus stars, the model-derived dust masses can be reproduced to within a factor of 2 for 60% of the stars, and within a factor of 3 for 70% of the stars. (For sources with effective dust temperatures substantially greater than 20 K, the single component dust model will overestimate the disk mass since $M_{\text{dust}} \propto T_{\text{dust}}^{-1}$). Assuming that the disk temperatures in the IC 348 cluster are not vastly different than in Taurus, adopting a dust temperature of 20 K, while simplistic, should reproduce the disk masses within a factor of a few for the majority of the stars. For these assumptions, the 3σ upper limit to the circumstellar disk mass around an individual star in the IC 348 cluster is $0.025 M_{\odot}$. Treating the 95 cluster members as an ensemble, the observed average flux corresponds to an average disk mass of $0.002 \pm 0.001 M_{\odot}$.

5. Discussion

The limits on the disk masses in the IC 348 cluster can be compared to disk masses in other star forming regions as a step toward determining the evolution of disk masses as a function of time and environment (e.g. “clustered” vs. “isolated” star formation). The Taurus star forming region provides a meaningful comparison since it has been thoroughly studied in the millimeter continuum (Beckwith et al. 1990; Osterloh & Beckwith 1995; see also Skinner, Brown, & Walter 1991 and Henning et al. 1998), and the stellar population has an age similar to IC 348 as shown below. Since the IC 348 sample has been identified largely based on spectroscopy, only stars in Taurus with spectral types and sufficient photometric information to place the stars on the HR diagram were used for this comparison. From the database of spectral types and photometry compiled from the literature by Hillenbrand, Meyer, & Carpenter (2002), 117 stars were identified in Taurus that met these criteria and have a published $\lambda 1.3\text{mm}$ continuum flux measurement. The main source of incompleteness in the Taurus sample are deeply embedded IRAS sources which are not detected at optical wavelengths (Kenyon & Hartmann 1995), and recently identified low mass stars and brown dwarfs (Briceño et al. 1998,99; Luhman & Rieke 1998) that have not yet been surveyed in the millimeter continuum.

The open histograms in the top panels of Figures 2 and 3 show the mass and age distributions respectively for the Taurus comparison sample. (The bottom panels show the analogous distributions for the IC 348 sample as already discussed.) The mean stellar mass of the Taurus sample is $\log_{10} (\text{mass}/M_{\odot}) = -0.33$ with a dispersion of 0.27. By comparison, the IC 348 sample has a mean \log_{10} stellar mass of -0.53 with a dispersion of 0.44. Therefore, the stellar mass distribution in IC 348 is skewed toward smaller stellar masses compared to the Taurus sample. Similarly, the mean stellar age of the Taurus sample is $\log_{10} (\text{age}/\text{yr}) = 6.0$ with dispersion of 0.6, while the mean \log_{10} age and dispersion for IC 348 are 6.3 and 0.6 respectively. Thus the stellar ages for IC 348 are skewed toward older values than stars in Taurus. However, the uncertainty in the distances to the star forming regions, which is at least $\sim 10\%$, (Kenyon, Dobrzycka, & Hartmann 1994; de Zeeuw et al. 1999), will produce a ~ 0.09 dex uncertainty in the mean age (Hartmann 2001). At best then

the difference in the mean ages between Taurus and IC 348 are significant at the $\sim 2\sigma$ confidence level.

Disk masses for stars in Taurus were re-computed from published $\lambda 1.3\text{mm}$ fluxes and using the isothermal dust model adopted here for consistency. The hatched histograms in Figures 2 and 3 show the distribution of stellar masses and ages for stars in Taurus that have disk masses in excess of $0.025 M_{\odot}$, which is the 3σ upper limit to the disk masses toward individual stars in IC 348. Figure 2 shows that in this Taurus sample, such disks masses are found only around stars more massive than $0.27 M_{\odot}$. While the lack of such massive disks around lower mass stars may simply be due to the relative lack of sources, only stars more massive than $0.27 M_{\odot}$ are used in the following comparison between Taurus and IC 348. In the Taurus sample, 14 of the 99 stars with stellar masses greater than $0.27 M_{\odot}$ have disk masses in excess of $0.025 M_{\odot}$. In IC 348, none of the 48 stars in the same stellar mass range have such disk masses. Using the two-tailed Fisher Exact Test, the probability that the frequency distribution of massive disks in IC 348 and Taurus have been drawn from the same parent population is 0.0028. This probability is independent of the assumed values of κ_o and T_{dust} used to compute the disk masses to the extent that the disk properties in the two regions are similar. However, if the value of β is as low as 0.5 on average (Beckwith & Sargent 1991; Mannings & Emerson 1994) as opposed to the assumed value of $\beta=1$, then the disk masses in IC 348 will be systematically overestimated compared to Taurus, and the difference in the frequency of massive disks will be enhanced. Thus despite the similar stellar ages of the star forming regions, the IC 348 cluster lacks the massive disks found in the Taurus at the $\sim 3\sigma$ confidence level. The cause of this apparent difference cannot be due to an photoevaporation of the disks in IC 348 from a high ultraviolet radiation field (e.g. Johnstone, Hollenbach, & Bally 1998) since the spectral type of the most massive cluster member in IC 348 is B5 (Luhman et al. 1998). Whether or not the difference in disk masses can be attributed to the affects of a “cluster” vs. “isolated” environment remains speculative given the limited sample of star forming regions, although continuum surveys of additional clusters are possible with current interferometers.

The IC 348 results can also be compared to the disk masses in Orion Nebula Cluster using the 86 GHz continuum survey by Mundy, Looney, & Lada (1995). Again using a 20 K dust temperature for consistency with the assumptions adopted here, the 3σ upper limit to individual disk masses in Orion is $0.17 M_{\odot}$. Mundy, Looney, & Lada (1995) derived a 95% upper limit to the characteristic flux at 86 GHz of 1.1 mJy, which corresponds to a disk mass of $0.03 M_{\odot}$. Thus the results from Mundy, Looney, & Lada (1995) exclude the presence of massive disks in Orion, but do not set as stringent limits as the IC 348 observations for disk masses in cluster environments. Similarly, Bally et al. (1998) derived a 3σ upper limit of $0.015 M_{\odot}$ to the disk mass around 5 proplyds in the Orion Nebula cluster for an assumed dust temperature of 50 K. If a 20 K dust temperature is instead adopted, the corresponding upper limit is $0.047 M_{\odot}$.

Finally, the IC 348 results can be contrasted with the minimum disk mass needed to form the Solar System. Summing the mass contained in the planets and assuming an interstellar gas to dust ratio, the minimum mass of the primitive solar nebula is $\sim 0.01 M_{\odot}$ (Weidenschilling 1977; Hayashi

1981). This minimum mass reflects primarily the mass needed to form a Jupiter-mass planet. The actual mass of the primitive solar nebula may of course be higher depending on the efficiency in converting dust and gas in the primitive solar nebula into planets. The upper limit to the typical disk mass in IC 348 is comparable then to the minimum mass of the solar nebula, and the average mass is ~ 5 times lower than minimum mass of the solar nebula. Given that the disk masses are uncertain by at least a factor of 3 due the mass opacity coefficient (κ_o), these results suggest either that the formation of planets with masses greater than a few Jupiter masses is relatively rare around 0.2-0.5 M_\odot stars in IC 348, or that the formation of gas-giant planets has significantly depleted the disk of small dust grains on a time scale of $\lesssim 2$ Myr, the mean age of the IC 348 cluster.

6. Summary

I present OVRO observations of a $5.2' \times 5.2'$ region toward the IC 348 stellar cluster that has been imaged in the 98 GHz continuum to a RMS noise level of $0.75 \text{ mJy beam}^{-1}$ at $4.0'' \times 4.9''$ resolution. A total of 95 known members of the IC 348 cluster brighter than $K_s=14.5$ are located within the mosaicked region. The stellar masses range from $0.03 M_\odot$ to $4.2 M_\odot$ with a peak in the distribution between $0.2 M_\odot$ and $0.5 M_\odot$. At least 15% of these stars are surrounded by an optically thick, inner accretion disk as evidenced by a $K_s - L$ excess (see Haisch, Lada, & Lada 2001a). The OVRO observations are used to place constraints on the circumstellar disk masses and provide a snapshot of disk evolution in a cluster environment at an age of ~ 2 Myr (Luhman 1999).

None of the 95 IC 348 members within the OVRO mosaic were detected at the 3σ level or greater. The mean flux toward the 95 stars is $0.22 \pm 0.08 \text{ mJy}$, indicating the observed fluxes are consistent with random noise although with a slight bias toward positive fluxes. The millimeter-wave continuum fluxes were converted into disk masses (the sum of the gas and dust components) assuming a dust temperature of 20 K, a mass opacity coefficient of $0.02 \text{ cm}^2 \text{ g}^{-1}$ at $1300 \mu\text{m}$, and a power law index for the particle emissivity of $\beta=1$. For any individual source, the 3σ upper limit to the circumstellar disk mass is $0.025 M_\odot$. For the 95 sources as an ensemble, the average disk mass is $0.002 \pm 0.001 M_\odot$.

The constraints placed on the disk masses in the IC 348 cluster were compared to the disk masses around stars in the Taurus molecular cloud. A subsample of the Taurus population was identified that has available optical spectroscopy and photometry as well as published millimeter continuum observations. The stellar mass range was restricted to stars with masses in excess of $0.27 M_\odot$ since that is the lowest mass star in the Taurus sample that has an observed disk mass in excess of $0.025 M_\odot$. In the Taurus sample, 14 of the 99 stars with stellar masses $\geq 0.27 M_\odot$ have disk masses in excess of $0.025 M_\odot$, while in IC 348, none of the 48 stars in the same stellar mass range have such disk masses. The probability that the frequency distribution of massive disks in IC 348 and Taurus have been drawn from the same parent population is 0.0028, and are thus different at the $\sim 3\sigma$ confidence level. These results suggest that the IC 348 stellar population lacks the massive disks that characterizes $\sim 14\%$ of the Taurus population despite the fact that the two regions have

similar ages (Hillenbrand, Meyer, & Carpenter 2002). Whether or not the differences between the frequency of massive disks between Taurus and IC 348 is related to “isolated” versus “clustered” star forming environments awaits observations of additional star forming regions.

The implications of the IC 348 observations for planet formation can be placed in context with the minimum mass of the primitive solar nebula ($\sim 0.01 M_{\odot}$; Weidenschilling 1977, Hayashi 1981) needed to form our Solar System. The IC 348 results suggest that if an optically thick accretion disk is the necessary seed to form gas-giant planets, then either few stars in IC 348 with stellar masses between $0.2 M_{\odot}$ and $0.5 M_{\odot}$ will form planets more massive than a few Jupiter masses, or the process to form such massive planets has significantly depleted the disk of small dust grains by the age of the IC 348 cluster, or ~ 2 Myr.

JMC acknowledges support from Long Term Space Astrophysics Grant NAG5-8217 and the Owens Valley Radio Observatory, which is supported by the National Science Foundation through grant AST-9981546. This publication makes use of data products from the Two Micron All Sky Survey, which is a joint project of the University of Massachusetts and the Infrared Processing and Analysis Center, funded by the National Aeronautics and Space Administration and the National Science Foundation. 2MASS science data and information services were provided by the InfraRed Science Archive (IRSA) at IPAC.

REFERENCES

Adams, F. C., Shu, F. H., & Lada, C. J. 1988, *ApJ*, 326, 865

André, P. & Montmerle, T. 1994, *ApJ*, 420, 837

Bally, J., Testi, L., Sargent, A., & Carlstrom, J. 1998, *ApJ*, 116, 854

Beckwith, S. V. W., Sargent, A. I., Chini, R. S., & Güsten, R. 1990, *AJ*, 99, 924

Beckwith, S. V. W., & Sargent, A. I. 1991, *ApJ*, 381, 250

Bessell, M. S., & Brett, J. M. 1988, *PASP*, 100, 1134

Boss, A. P. 2001, *ApJ*, 563, 367

Briceño, C., Calvet, N., Kenyon, S., & Hartmann, L. 1999, *AJ*, 118, 1354

Briceño, C., Hartmann, L., Stauffer, J., & Martín, E. 1998, *AJ*, 115, 2074

Calvet, N., Patiño, A., Magris, G. C., & D'Alessio, P. 1991, *ApJ*, 380, 617

Calvet, N., Magris, G. C., Patiño, A., & D'Alessio, P. 1992, *Rev. Mex. Astron. Astrofis.*, 24, 27

Carpenter, J. M. 2000, *AJ*, 120, 3139

_____ 2001, *AJ*, 121, 2851

Chiang, E.I., & Goldreich, P. 1997, *ApJ*, 490, 368

Cohen, J. G., Grogel, J. A., Perrson, S. E., & Elias, J. H. 1981, *ApJ*, 249, 481

D'Antona, F., & Mazzitelli, I. 1997, *Mem. Soc. Astron. Italiana*, 68, 807

D'Antona, F., & Mazzitelli, I. 1998, ASP conf. ser. 134, “Brown Dwarfs and Extrasolar Planets”, eds. R. Rebolo, E. L. Martin, and M. R. Zapatero-Osorio (San Franciso: ASP), 442

de Zeeuw, P. T., Hoogerwerf, R., de Bruijne, J. H. J., Brown, A. G. A., & Blaauw, A. 1999, *ApJS*, 117, 354

Dutrey, A., Guilloteau, S., Duvert, G., Prato, L., Simon, M., Schuster, K., & Ménard, F. 1996, *A&A*, 309, 493

Haisch, K. E. Jr., Lada, E. A., & Lada, C. J. 2001a, *ApJ*, 553, L153

_____ 2001b, *AJ*, 121, 2065

Hartmann, L. 2001, *AJ*, 121, 1030

Hayashi, C. 1981, *Prog. Theor. Phys. Supp.* 1981, 70, 35

Henning, T., Burkert, A., Launhardt, R., Leinert, C., & Stecklum, B. 1998, *A&A*, 336, 565

Henning, T., Pfau, W., Zinnecker, H., & Prusti, T. 1993, *A&A*, 276, 129

Herbig, G. H. 1998, *ApJ*, 497, 736

Hildebrand, R. H. 1983, *QJRAS*, 24, 267

Hillenbrand, L. A., Meyer, M. R., & Carpenter, J. M. 2002, in preparation

Kenyon, S., J., Dobrzycka, D., & Hartmann, L. 1994, *AJ*, 108, 1872

Kenyon, S., J., & Hartmann, L. 1995, *ApJS*, 101, 117

Johnstone, D., Hollenbach, D., & Bally, J. 1998, *ApJ*, 499, 758

Lada, E. A., DePoy, D. L., Evans, N. J. II, & Gatley, I. 1991, *ApJ*, 371, 171

Lada, E. A., & Lada, C. J. 1995, *AJ*, 109, 1682

Luhman, K. L. 1999, *ApJ*, 525, 466

Luhman, K. L., & Rieke, G. H. 1998, *ApJ*, 497, 354

Luhman, K. L., Rieke, G. H., Lada, C. J., & Lada, E. A. 1998, *ApJ*, 508, 347

Lynden-Bell, D., & Pringle, J. E. 1974, *MNRAS*, 168, 603

Mannings, V., & Emerson, J. P. *MNRAS*, 267, 361

Marcy, G. W., Cochran, W. D., & Mayor, M. 2000, *Protostars and Planets IV*, eds. V. Mannings, A. P. Boss, and S. S. Russell, (Tucson:University of Arizona Press), 1285

Motte, F., & André, P. 2001, *A&A*, 365, 440

Motte, F., André, P., & Neri, R. 1998, *A&A*, 336, 150

Mundy, L. G., Looney, L. W., & Lada, E. A. 1995, *ApJ*, 452, L137

Nürnberger, D., Brandner, W., Yorke, H. W., & Zinnecker, H. 1998, *A&A*, 330, 549

Nürnberger, D., Chini, R., & Zinnecker, H. 1997, *A&A*, 324, 1036

Najita, J. R., Tiede, G. P., & Carr, J. S. 2000, *ApJ*, 541, 977

O'Dell, C. R., & Wong, S. K. 1996, *AJ*, 111, 846

Osterloh, M., & Beckwith, S. V. W. 1995, *ApJ*, 439, 288

Padgett, D. L., Brandner, W., Stapelfeldt, K. R., Strom, S. E., Terebey, S., & Koerner, D. 1999, *AJ*, 117, 1490

Pollack, J. B., Hubickyj, O., Bodenheimer, P., Lissauer, J. J., Podolak, M., & Greenzweig, Y. 1996, *Icarus*, 124, 62

Preibisch, T., & Zinnecker, H. 2001, *AJ*, 122, 866

Scally, A., & Clarke, C. 2001, *MNRAS*, 325, 449

Scoville, N. Z., Carlstrom, J. E., Chandler, C. J., Phillips, J. A., Scott, S. L., Tilanus, R. P. J., & Wang, Z. 1993, *PASP*, 105, 1482

Skinner, S. L., Brown, A., & Walter, F. M. 1991, *AJ*, 102, 1742

Skrutskie, M. F., Dutkevitch, D., Strom, S. E., & Strom, K. M. 1990, *AJ*, 99, 1187

Störzer, H. & Hollenbach, D. 1999, *ApJ*, 515, 669

Strom, K. E., Strom, S. E., Edwards, S., Cabrit, S., & Skrutskie, M. F. 1989, *AJ*, 97, 1451

Testi, L., & Sargent, A. I. 1998, *AJ*, 116, 854

Weidenschilling, S. J. 1977, *Ap&SS*, 51, 153

Wilking, B. A., Lada, C. J., & Young, E. T. 1989, *ApJ*, 340, 823

Wood, K., Lada, C. J., Bjorkman, J. E., Kenyon, S. J., Whitney, B., & Wolff, M. J. 2002, *ApJ*, in press

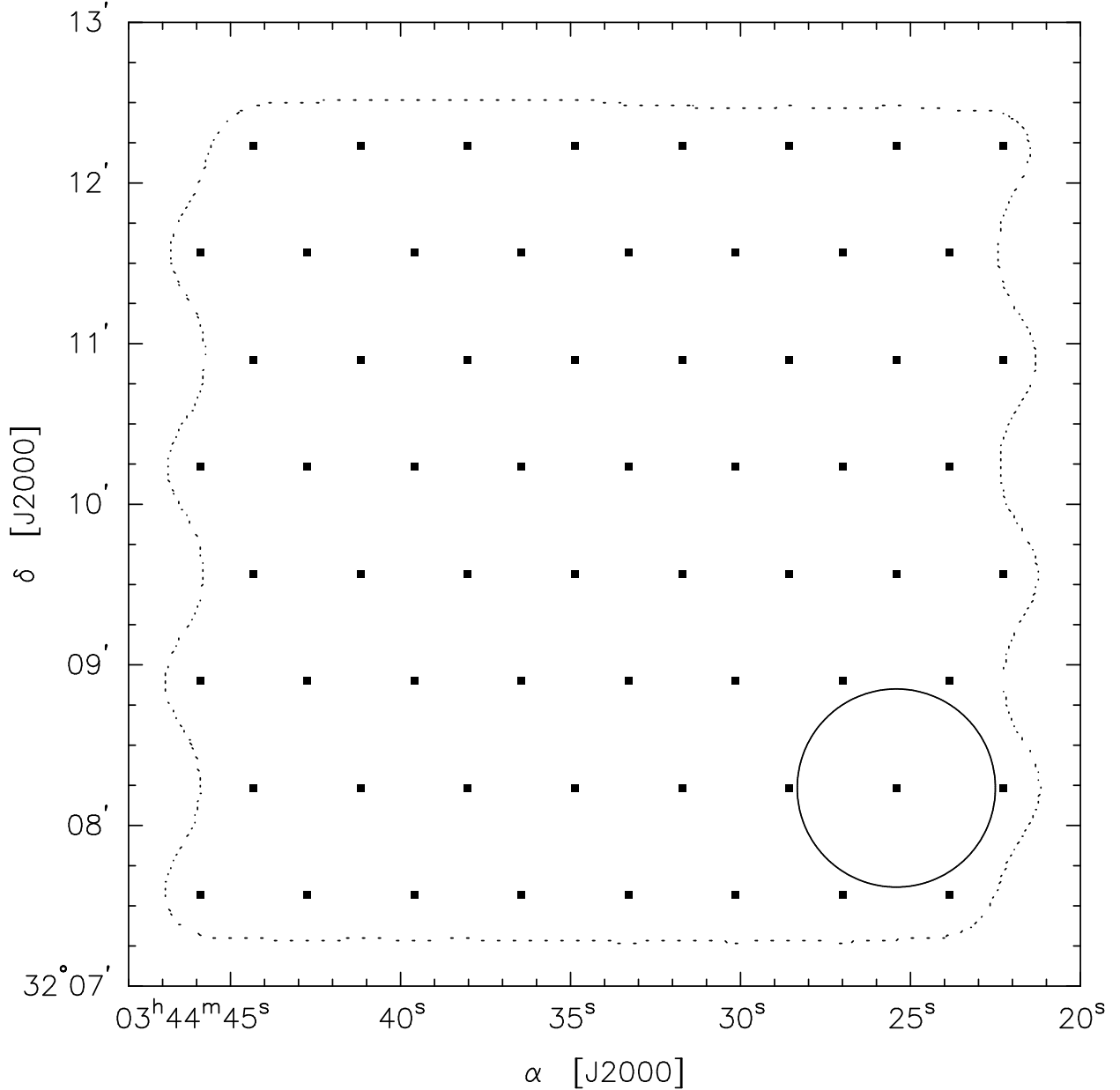


Fig. 1.— Schematic of the IC 348 mosaic made with OVRO. The solid squares mark the 64 pointing centers used to create the mosaic. The pointing centers are separated by $40''$ along a row, with adjacent rows also separated by $40''$. For comparison, the circle in the lower right corner shows the FWHM beam size of a single OVRO antenna (72'') at the observed frequency 98 GHz. The dotted curve shows the extent of the OVRO mosaic ($\sim 5.2' \times 5.2'$) at the unit gain boundary. The synthesized beam size is $4.0'' \times 4.9''$.

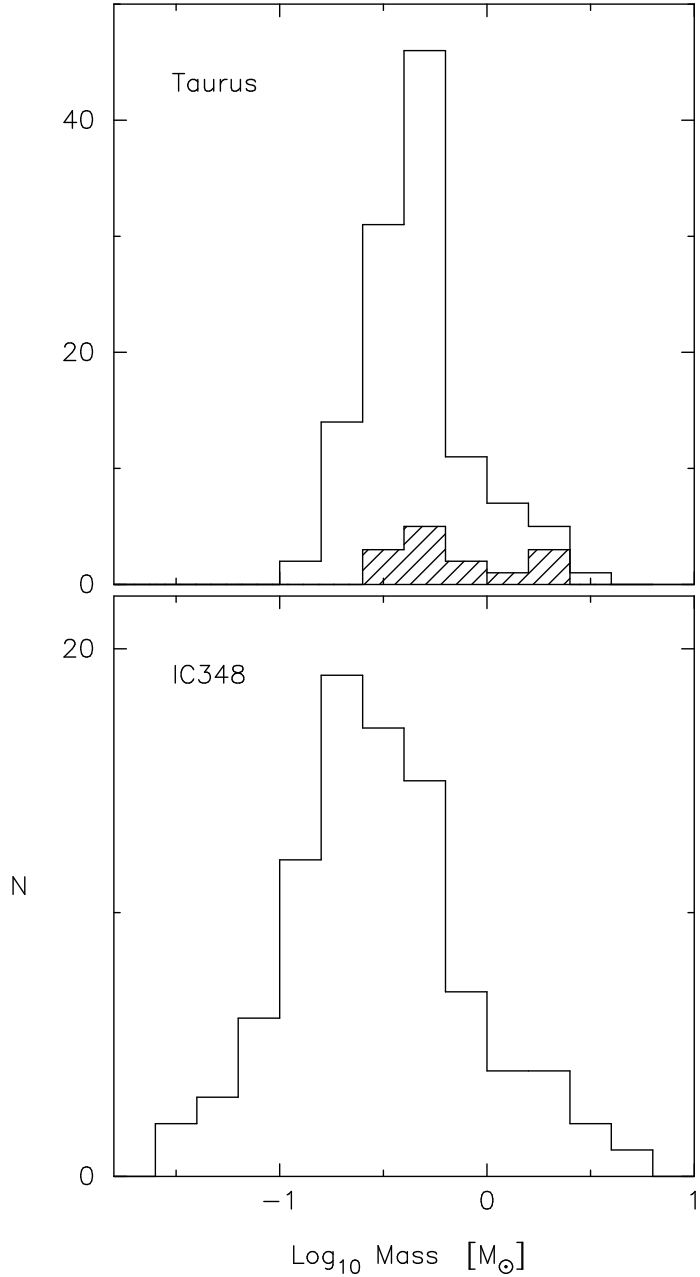


Fig. 2.— *Bottom*: Histogram of the stellar masses for the IC 348 cluster members located within the OVRO mosaic. Three probable IC 348 members within the OVRO mosaic did not have sufficient data to infer their stellar properties and are not shown in this figure. *Top*: Histograms of the stellar masses for a comparison sample of stars in the Taurus molecular cloud that have available optical spectroscopy, photometry, and submillimeter continuum observations. The open histogram represents all stars in the comparison sample, and the hatched histogram shows the stellar mass distribution for sources that have a disk mass greater than the 3σ detection limit of $0.025 M_{\odot}$ for the IC 348 observations. The stellar masses in both IC 348 and Taurus have been inferred by placing the stars in an HR diagram using the database compiled by Hillenbrand, Meyer, & Carpenter (2002) and the D'Antona & Mazzitelli (1997,98) pre-main-sequence evolutionary tracks.

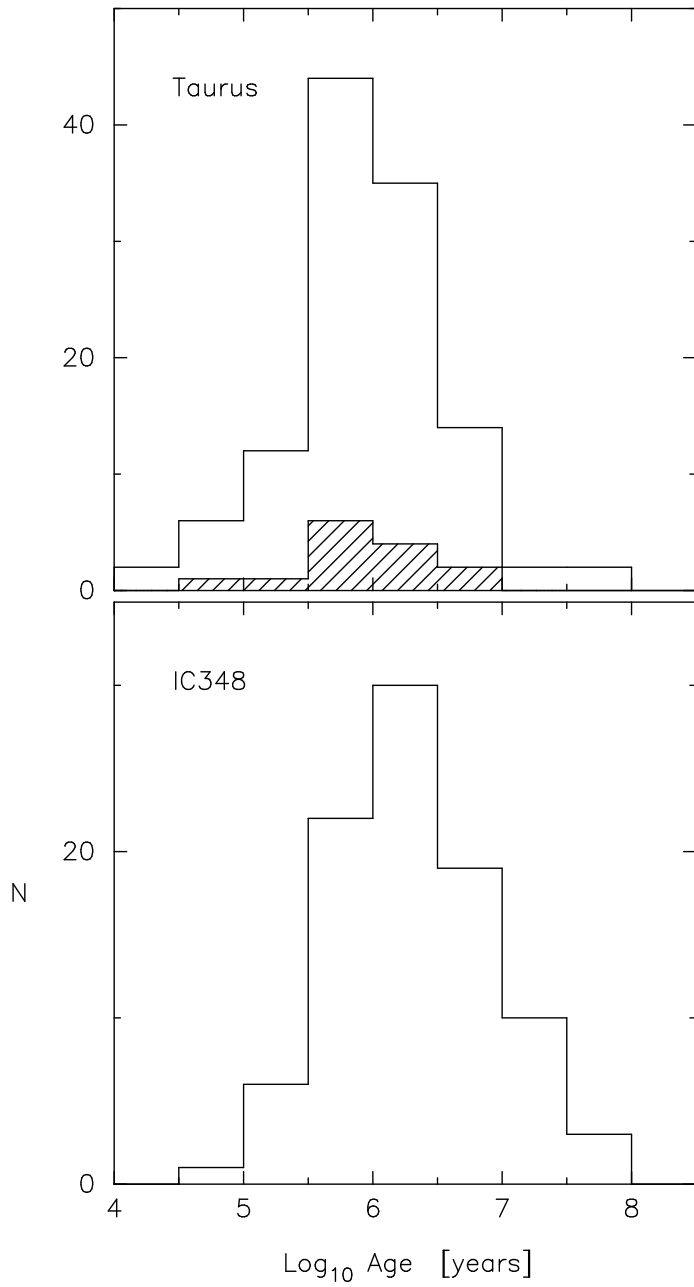


Fig. 3.— *Bottom*: Histogram of the stellar ages for the IC 348 cluster members within the OVRO mosaic. *Top*: Histograms of the stellar ages for a comparison sample of stars in the Taurus molecular cloud as described in Fig. 2.

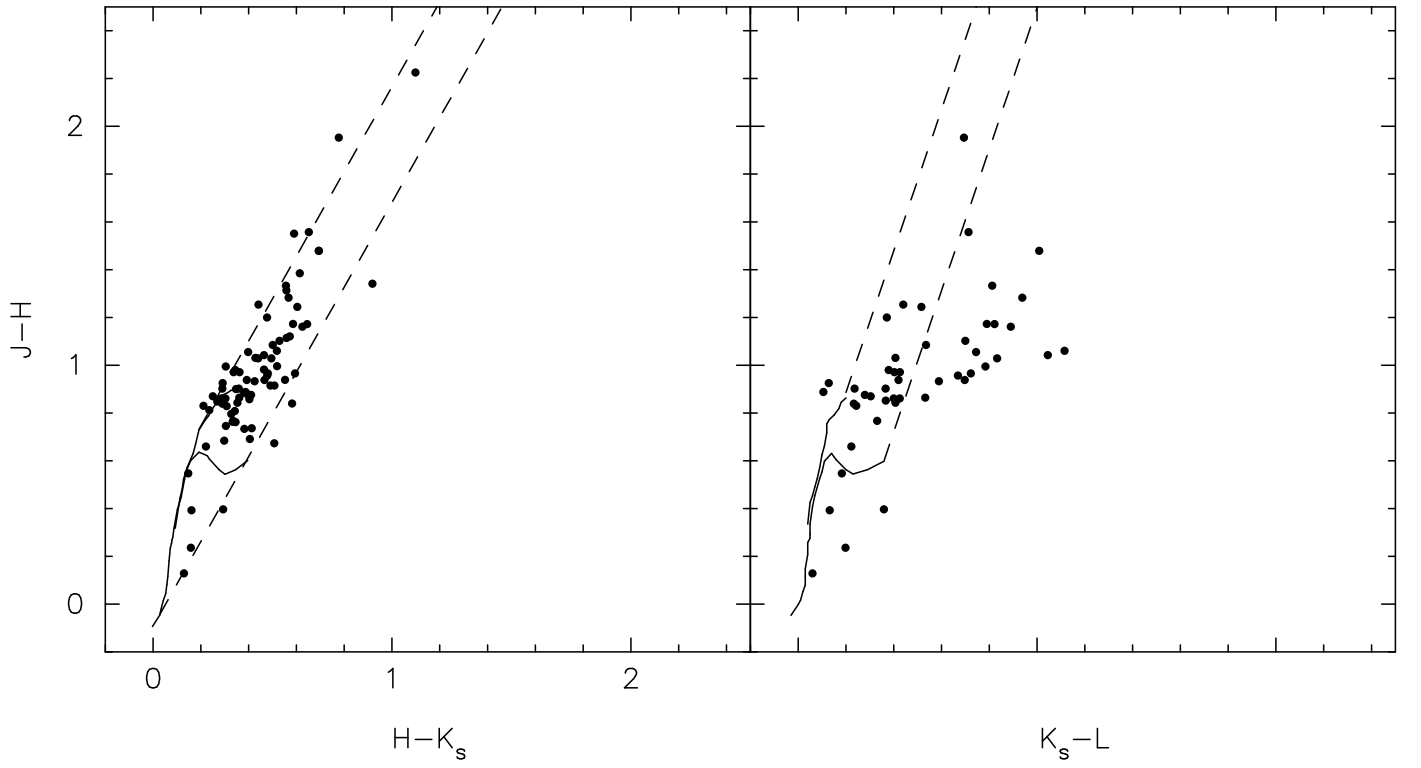


Fig. 4.— *Left:* $J - H$ vs. $H - K_s$ color-color diagram for 82 IC 348 members in the OVRO mosaic that have photometry in the 2MASS database without any error flags. *Right:* $J - H$ vs. $K_s - L$ color-color diagram for 47 IC 348 members in the OVRO mosaic with 2MASS photometry and L -band photometry from Haisch, Lada, & Lada (2001a). In each panel, the solid curves represent the locus of main-sequence and giant stars Bessell & Brett (1988) and the dashed line is the interstellar reddening vector (Cohen et al. 1981), where the $J - H$ and $H - K$ colors have been transformed into the 2MASS photometric system (Carpenter 2001). Four stars exhibit an apparent $H - K_s$ excess, but in each instance, the magnitude of the excess is less than the 1σ photometric uncertainties and can be attributed to photometric noise. In the $J - H$ vs. $K_s - L$ diagram, 18 stars show an apparent $K_s - L$ excess, of which 14 have an excess larger than the estimated photometric uncertainties. Therefore, a minimum of 15% of the 95 IC 348 cluster members within the OVRO mosaic contain a detectable $K_s - L$ excess indicative of an optically thick circumstellar disk.

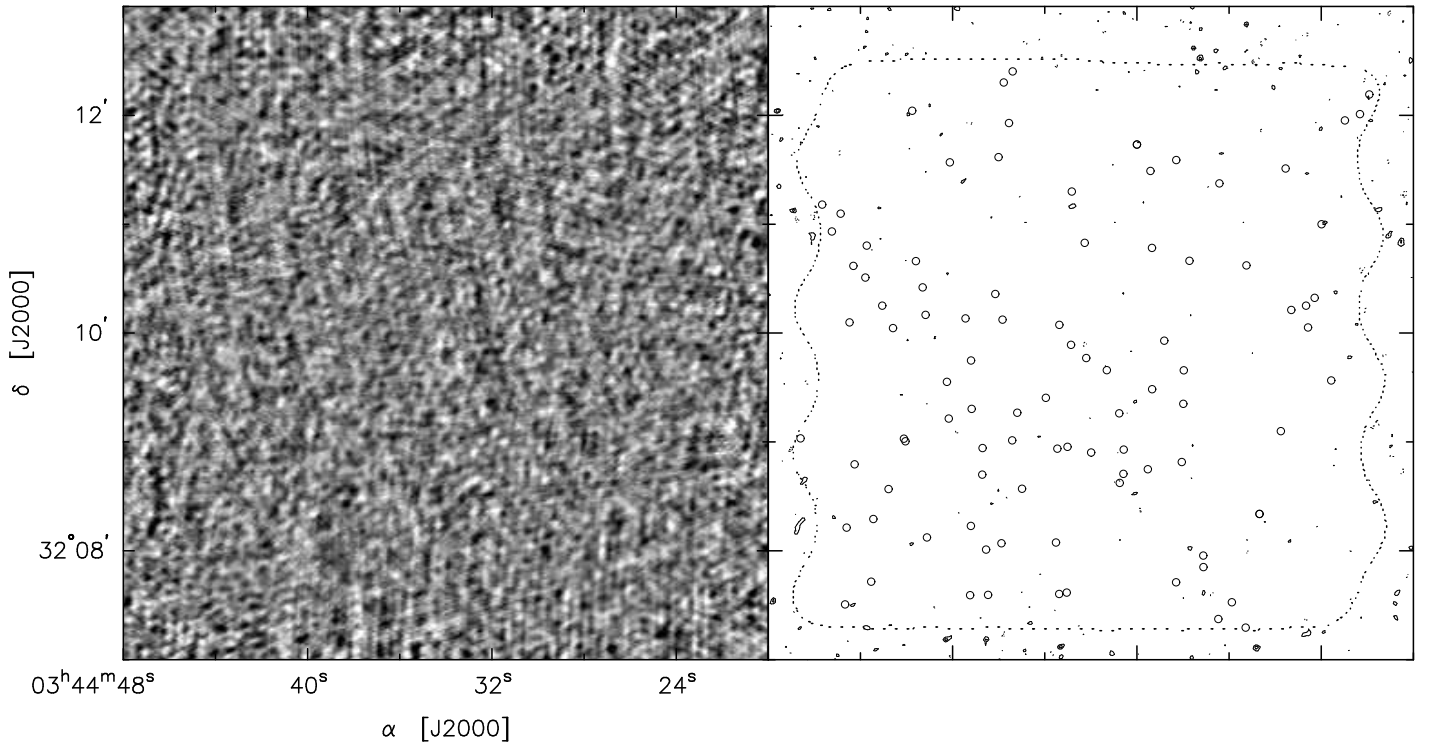


Fig. 5.— *Left:* Grayscale image of the $\lambda 3\text{mm}$ continuum emission toward IC 348. Darker regions represent bright intensities. *Right:* Contour map of the OVRO mosaic. Contours begin at 3σ above the RMS noise of $0.75 \text{ mJy beam}^{-1}$ with increments of 1σ . The dotted boundary that encompasses the image shows the unit gain boundary of the mosaic (see Fig. 1). Open circles represent 95 probable members of the IC 348 cluster within the field of view of the OVRO mosaic that have been identified from spectroscopy (Herbig 1998; Luhman et al. 1998; Luhman 1999) and narrow band imaging (Najita, Tiede, & Carr 2000). This figure shows that none of the known IC 348 stars were detected in the $\lambda 3\text{mm}$ continuum at the 3σ noise level or greater.

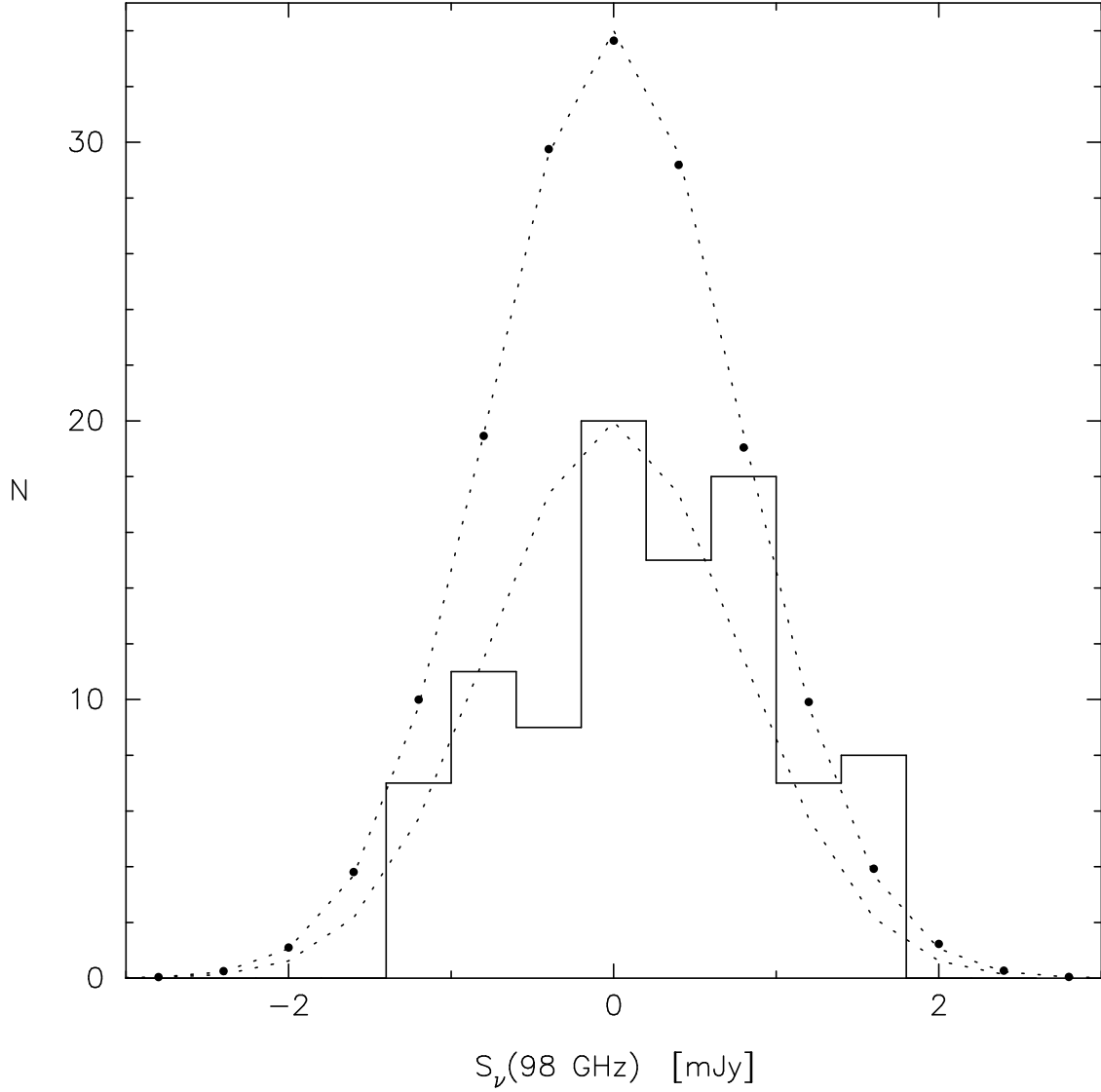


Fig. 6.— Frequency distribution of the observed flux densities at 98 GHz over the entire OVRO mosaic (solid circles) and toward the 95 IC 348 members (histogram). The frequency distribution indicated by the solid circles have been arbitrarily scaled by 1/600. The dotted curves through the circles and through the histogram show the expected distribution of fluxes in the two samples for gaussian noise with a dispersion of $0.75 \text{ mJy beam}^{-1}$, which is the average noise in the OVRO mosaic. This figure shows that the fluxes over the entire mosaic are consistent with gaussian noise. The mean flux observed toward the 95 IC 348 members is $0.22 \pm 0.08 \text{ mJy}$, where the uncertainty is the standard deviation of the mean.

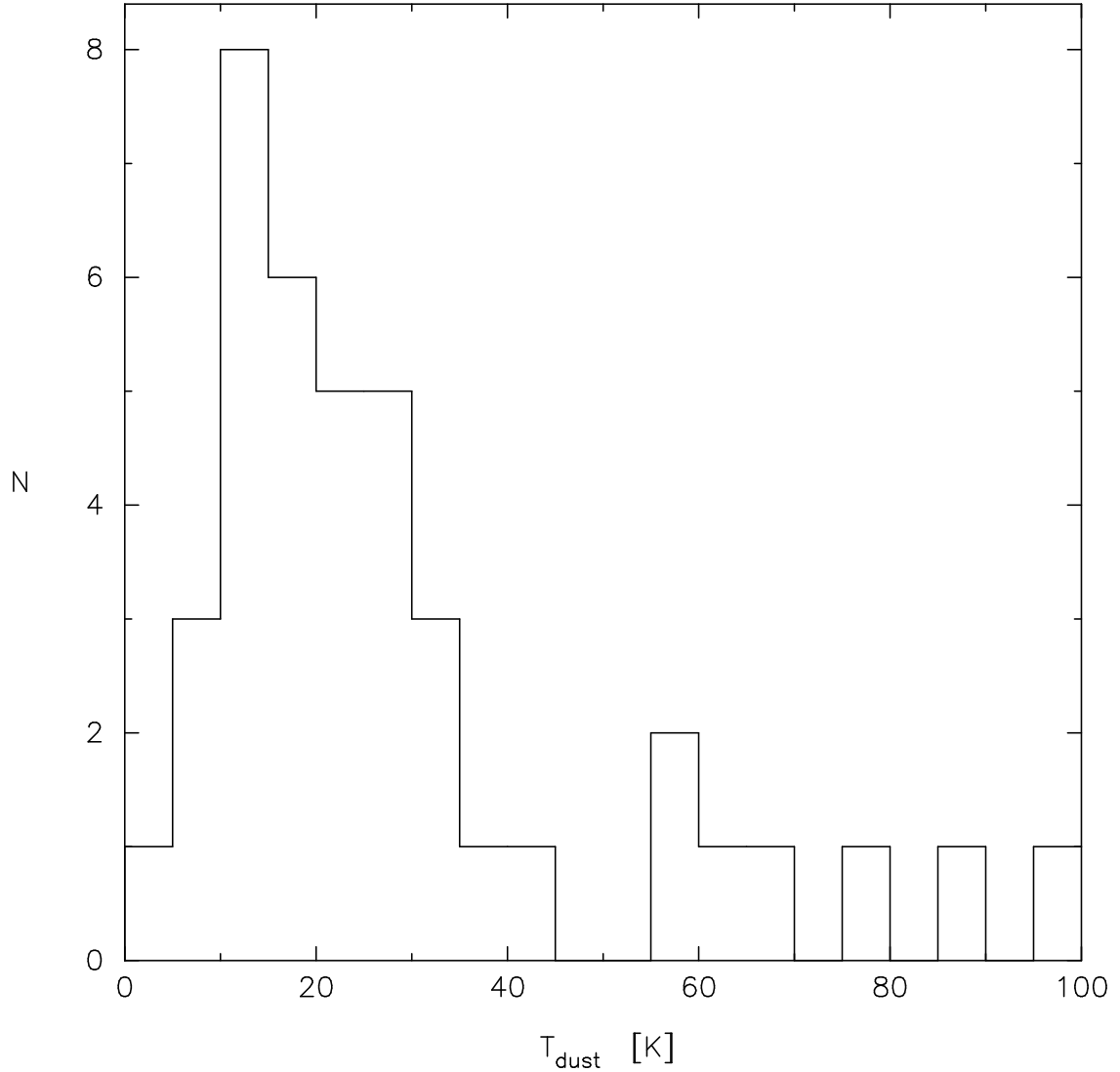


Fig. 7.— Histogram of the effective dust temperatures of circumstellar disks in Taurus-Auriga. The effective dust temperature represents the dust temperature that, when combined with the observed $\lambda 1.3\text{mm}$ fluxes, reproduces the disk masses derived by fitting power-law distributions for the dust temperature and mass surface density to the observed spectral energy distribution of young stars in Taurus-Auriga (Beckwith et al. 1990; Osterloh & Beckwith 1995). Most stars have effective dust temperatures of ~ 20 K, which was used to convert the observed OVRO $\lambda 3\text{mm}$ fluxes to disk masses. Four stars have effective dust temperatures greater than 100 K and are not shown in this figure.